Alkali metal adsorption on graphite: a review

2005 J. Phys.: Condens. Matter 17 R995

(http://iopscience.iop.org/0953-8984/17/35/R02)

INSTITUTE OF PHYSICS PUBLISHING JOURNAL OF PHYSICS: CONDENSED MATTER

J. Phys.: Condens. Matter **17** (2005) R995–R1024 doi:10.1088/0953-8984/17/35/R02

TOPICAL REVIEW

Alkali metal adsorption on graphite: a review

Mellita Caragiu[1] **and Sharon Finberg**[2]

[1] Department of Physics and Astronomy, Ohio Northern University, 525 S Main Street, Ada, OH 45810, USA
[2] Department of Natural Sciences, Bentley College, 175 Forest Street Waltham, MA 02452, USA

E-mail: m-caragiu@onu.edu and SFINBERG@bentley.edu

Received 1 May 2005, in final form 12 July 2005
Published 19 August 2005
Online at stacks.iop.org/JPhysCM/17/R995

Abstract

The adsorption of alkali metals on graphite has been the subject of various studies for the past two decades. Briefly, two main reasons can be offered to justify the persisting interest in these adsorption systems. First, experiments have pointed out intriguing structural phase transitions of the adsorbed species, and, second, in an attempt to explain the experimental results, the more complicated question of the nature of alkali metal–graphite bonding arose. Despite the relative simplicity of the electronic structure of the alkali metals, their interaction with the graphite surface is still the subject of current debate. This review paper presents relevant experimental data and results of selected theoretical calculations that, in time, guided the process of scientific discovery towards the current understanding of the alkali metals/graphite adsorption systems.

Contents

1. Introduction

Prior to writing an overview on the topic of alkali metals interacting with graphite surfaces, one starts by asking why this particular subject has kept the interest of scientific researchers alive for more than 15 years. The answer must be the existence of some controversial results that wait for clarification and in the meantime fuel the efforts of experimentalists and theoreticians.

Graphite is a highly anisotropic material in terms of its structural and electric properties, due to relatively strong in-plane forces between the carbon atoms, but weak interplanar forces between adjacent graphene layers. It is no wonder, therefore, that atoms of various chemical species intercalate within the graphite surface, forming atomic or molecular layers. The interest in these intercalation compounds is due to the change in electronic and mechanical properties of the host induced by the intercalates, which ensures diverse technological applications of the new materials.

At the same time, alkali metals (highly reactive chemical species) have a fairly simple electronic configuration and can act as potential donors when intercalated within graphite, thus easily changing the concentration of free carriers of graphite and, therefore, the properties of the substrate. For this reason, alkali metals intercalated within a graphite substrate have been the subject of thorough investigation for the past 20 years [1]. The studies recorded a boost when connected to the fairly new field of fullerenes, since alkali-doped C_{60} compounds have proven to exhibit outstanding mechanical and electrical properties. In spite of the research, there are still aspects mainly related to the kinetics of the intercalation process (mechanism of intercalation, intercalation sites, change of the rate of intercalation with various parameters) that need explanation.

Still, alkali metal atoms do not always form intercalation compounds. Upon deposition on graphite, these atoms adsorb on the surface either as a diffuse layer or as a two-dimensional commensurate superstructure. There are certain features in the phase diagrams of the alkali metal/graphite systems that can be regarded as unusual in comparison with the structures formed by the same atoms adsorbed on other substrates. For instance, the abrupt transition between certain structural phases that takes place at a particular adsorbate coverage constitutes a deviation from the expected smooth increase in density of one phase as the coverage increases. Also, the fact that certain alkali metals exhibit high predisposition towards intercalation within the graphite surface but have not been found to form ordered overlayers should be properly addressed. Similarly, it has been known that other alkali metal atoms rarely form intercalation compounds. And, of course, there is the problem that different crystallographic structures have been occasionally obtained under similar experimental conditions. Since the structural order is dictated, ultimately, by the electronic interaction between the alkali metal atom and the graphite substrate, an attempt to solve the above-mentioned problems poses another question: the nature of the alkali metal–graphite bond. The investigation of the electronic charge transfer between the adsorbate and substrate is expected to elucidate the character of the K–graphite bond: whether it is an ionic bonding or a metallic one, a problem which is still under much debate. Due to the relative simplicity associated with the electronic structure of both alkali metal and

graphite—the alkali metal atoms are hydrogen-like while the graphite can be treated, in a first approximation, as a two-dimensional system—it is possible to perform electronic structure calculations for this system. The coordination of experiments and theoretical calculations is expected to ultimately form a coherent image of the alkali metal–graphite adsorption systems.

2. General considerations

Certain combinations of various factors will determine either a unique crystallographic structure of the adsorbed alkali metal on graphite, or, alternatively, its intercalation within the graphite layers. These factors are: the coverage of alkali atoms, the temperature at which the deposition takes place as well as the post-dose annealing temperatures, and the initial condition of the substrate. Each parameter will be briefly discussed in the following, in order to give a general idea about the customary experimental conditions.

There are basically two choices for selecting graphite samples as substrates for alkali metal adsorption experiments: single-crystal graphite (SCG), or highly oriented pyrolytic graphite (HOPG). The main difference between the two types of graphite is in their structural order. SCG exhibits a high structural order for the spatial extension of one crystal flake which is, unfortunately, not too large: approximate dimensions are 1 mm radius and several tens of hundredths of a millimetre thickness [1]. SCG samples are found in nature, as a result of mining. HOPG is a polycrystalline graphite synthetically obtained by applying high temperature and pressure to a hydrocarbon. It consists of grains which are composed, in turn, of crystallites: stacked hexagonal carbon layers. The statistical orientation of the grains and their crystallites determines the properties of the HOPG sample. In general, the grains are oriented along the c-axis of the crystal within a 1° tolerance, while the crystallites (of approximate dimension of 1 μm) are arranged in a disorderly fashion along the a-axis of the crystal [1, 2].

The concentration of defects present on the surface of the graphite crystal is of great importance for the adsorption and intercalation of alkali atoms on graphite. Both SCG and HOPG surfaces exhibit monoatomic steps, which translate into both A and B terminations of the topmost carbon layer. Using single-crystal natural graphite it is possible to find small regions which are virtually devoid of monoatomic steps [3], but the common case is one where the graphite surface exhibits significant numbers of these defects, more so for HOPG than for SCG samples. A generally accepted value for the density of steps is 10^8 cm^{-2} [4, 5].

The coverage of the adsorbed atoms has a major influence upon the structure of the overlayer. The particular example of K adsorbed on graphite will be used to illustrate several different ways to define the coverage.

The research papers in this area often use the density of atoms that form a close-packed layer as a measure of one monolayer of that particular atomic species. For instance, taking the K radius to be 2.31 Å (the metallic radius), a close-packed K layer would roughly accommodate 5.4×10^{14} atoms cm^{-2}. Nevertheless, a density of 5.2×10^{14} atoms cm^{-2} is generally accepted as the equivalent of one K monolayer, since it represents the density of close-packed K atoms on metals [6]. This latter value will therefore be occasionally encountered in scientific papers to describe one K monolayer (1 ML), or $\theta = 1$ [7, 8]. Similarly, one monolayer occasionally refers to the density of atoms of the bcc(110) surface of the alkali metal in its bulk structure. This surface is only quasi-hexagonal, but similar to the hexagonal arrangement of the graphite substrate [4, 9].

A common definition for 1 ML of adsorbate uses the idea of the most densely packed phase that the adatoms form on the given surface. In the case of K on graphite, this would be the (2×2) phase, in which one K atom corresponds to 8 C atoms; it is this arrangement, therefore, that defines one monolayer of adsorbed K [5, 10–12]. According to this convention,

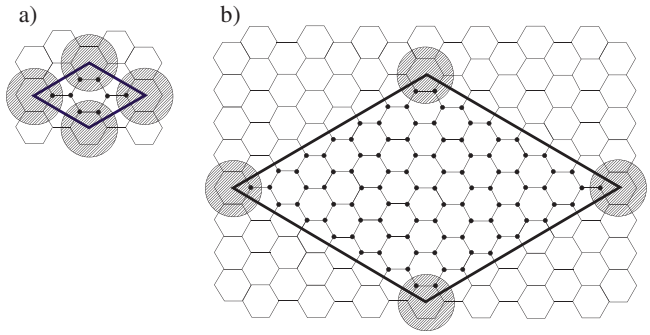

Figure 1. Model structure for (a) graphite (0001)-(2 × 2)-AM and (b) graphite (0001)-(7 × 7)-AM. The big circles represent the alkali metal (AM) atoms and the small black dots inside the overlayer unit cell represent the C atoms. One AM atom corresponds to 8 C atoms in the (2 × 2) structure and to 98 C atoms in the (7 × 7) structure.

another, less dense structure, such as (7 × 7), with one K atom corresponding to 98 C atoms, would imply a coverage of $8/98 \times 1$ ML ≈ 0.08 ML. Figure 1 shows both the (2 × 2) and the (7 × 7) structures formed by an alkali metal on graphite, and stresses the number of C atoms (little dark dots) comprised in one overlayer unit cell.

Taking the radius of the C atoms as 0.71 Å, the density of C atoms in the basal plane of graphite (0001) becomes 38.2×10^{14} atoms cm^{-2}. Since in a (2 × 2) K overlayer one K atom corresponds to eight C ones, the K surface density represents 1/8th of the C density, and therefore a value of 4.8×10^{14} K atoms cm^{-2}. In this way, 1 ML of K can also be referred to as a 4.8×10^{14} atoms cm^{-2} density of alkali metal atoms.

Yet another way to define coverage is by taking the ratio of the adatoms on the surface to the number of C atoms in a surface layer [13, 14]. In this case, a (2 × 2) structure with one adatom corresponding to eight C atoms, would correspond to a $1/8 = 0.125$ coverage. One can also express the density of adsorbed atoms on graphite using the ratio of the number of adsorbed atoms per graphite unit cell [15, 16]. Consequently, a coverage of 0.25 is assigned to the (2 × 2) overlayer since one adatom is shared by four substrate unit cells.

The number of ways in which the coverage can be defined does not end here. It is, nevertheless, useful to try to report the structural changes of the overlayers and at the same time refer to a standardized definition of coverage. Since the largest number of articles define 1 ML as the coverage of the highest-density overlayer structure, this is the understanding throughout the rest of this paper. Exceptions will be made for the adsorption systems for which the most densely packed structure is not definitely known, such as Cs/graphite, in which cases the particular definition for 1 ML will be stated at the appropriate place.

Due to the multitude of experiments that provide useful and complementary information about the alkali metals adsorbed on graphite, the description of the experimental methods is left to individual papers. Still, since the object of study is an adsorption system, in all cases ultrahigh vacuum conditions are required, and all studies start with the deposition process.

Ordinarily, the alkali metals are evaporated from well-degassed getter sources (SAES getters) by passing a high current (5–7 A) through them, for well-defined time periods. The alkali source is mounted on a collimated holder and the deposition is controlled by the use of a shutter kept open for the duration of the deposition. Depending on the actual geometry of the arrangement of alkali dispenser and graphite substrate, on the intensity of the electric current producing the alkali metal evaporation, and on the graphite temperature during dosing,

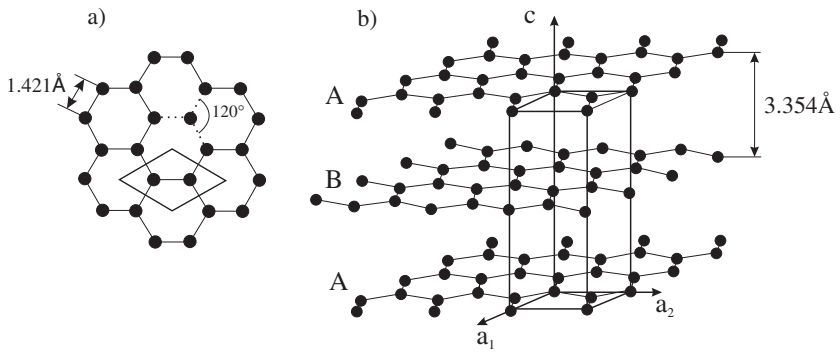

Figure 2. Model of (a) two-dimensional and (b) three-dimensional graphite together with the structural parameters. In (a), the surface unit cell, containing two C atoms, is highlighted.

a deposition time varying from several seconds to eight minutes is needed to produce the desired structures [9–12, 16–21].

Less frequently, the alkali source consists of the pure alkali metal sealed in a glass ampoule which is broken *in situ* and heated at a well-defined temperature in order to facilitate the evaporation of the substance. In this case, the temperature of the alkali source is known and can be kept constant during evaporation, representing a way to control the deposition rate and coverage. As an example, the time for depositing one K atomic layer could thus be varied from 1 to 9 min [22].

The techniques for monitoring and calibrating the adsorbate coverage are various and can be used concurrently to provide complementary information: Auger electron spectroscopy (AES)—which in principle compares the C and the alkali metal signals; quartz-crystal microbalance (QCM)—relating the shift in the oscillating frequency of a quartz crystal to the mass deposited on it; and low-energy electron diffraction (LEED)—providing a visual pattern of any ordered structure formed upon adsorption. Additional information about the coverage can be obtained from thermal desorption spectroscopy (TDS), work function measurements and high-resolution electron energy loss spectroscopy (HREELS).

The dosing temperature represents the temperature of the graphite substrate during the deposition process. The substrate can be maintained at various temperatures by mounting it on, usually, a copper block which in turn is connected to the cold finger of a cryostat. In this way, temperatures as low as 25 K [19] have been achieved and maintained for the duration of the experiments. For annealing purposes the sample can be resistively heated up to 1300 K and subsequently cooled down to the required deposition temperatures.

3. Structural study of single-crystal graphite and highly oriented pyrolytic graphite

Graphite is formed by carbon atoms with an sp^2 hybridization, each bound to three equidistant nearest neighbours 120° apart, forming hexagons with a side of 1.421 Å. These hexagonal structures connect in, theoretically, an infinite planar structure called graphene. If the stacking of the graphene planes follows the sequence ABAB . . ., then graphite crystals are formed. The vertical interplanar distance at room temperature is 3.354 Å [23]. Figure 2 shows models of two- and three-dimensional graphite along with the structural parameters.

As mentioned in section 2, both types of graphite—the single-crystal graphite (SCG), and the highly oriented pyrolytic graphite (HOPG)—have been used as substrates for alkali metal

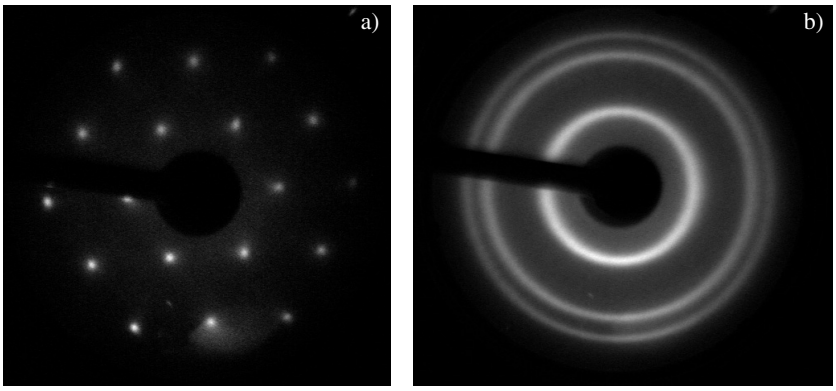

Figure 3. LEED patterns at 266 eV for clean (a) single-crystal graphite and (b) highly oriented pyrolytic graphite, obtained by Ferralis *et al* [21].

Table 1. Structural parameters for clean SCG and HOPG resulting from LEED $I(E)$ calculations [25, 21].

Parameter	SCG(0001) [25]	HOPG(0001) [21]
Sample temperature (K)	131	73
$d(C_1–C_2)$ (Å)	3.37 ± 0.04	3.35 ± 0.05
$d(C_2–C_3)$ (Å)	3.40 ± 0.06	3.36 ± 0.10
$d(C_3–C_4)$ (Å)	3.32 ± 0.08	3.31 ± 0.13

adsorption. Since this choice exists, a natural question arises: are there any differences between the SCG and the HOPG, and if so, how do the differences affect the adsorption process?

Both clean graphite substrates have been investigated by low-energy electron diffraction [3, 17, 21, 24, 25]; therefore it is meaningful to point out the differences between the diffraction pattern of an SCG sample and the one corresponding to an HOPG sample, shown in figure 3.

The azimuthal randomness of the crystallites that compose HOPG contrasts the high structural order characteristic to SCG and causes the diffraction spots of an SCG LEED pattern to be replaced by rings. The disadvantage of analysing a ring pattern is obvious: it becomes more difficult to determine the intensity of individual rings if these happen to be closely spaced, which makes a typical LEED structural determination more inaccurate.

The presence of monoatomic steps on the surface of the SCG and the HOPG as well, determines both A and B terminations of the topmost carbon layer. As a consequence, the LEED patterns posses an apparent sixfold symmetry (see figure 3), instead of the threefold symmetry which would occur if only one of the two terminations was present on the graphite surface.

Some of the structural parameters obtained upon performing full dynamical LEED calculations for the two graphite surfaces are presented in table 1. The notation $d(C_1–C_2)$ refers to the distance between the first two graphite layers; $d(C_2–C_3)$ and $d(C_3–C_4)$ have similar meaning.

In conclusion, the surface structure of clean SCG was found to be the same as that of HOPG and consistent with the bulk structure of graphite. The calculated interlayer spacings match the bulk value of 3.35 Å within the precision of the experiment. As expected, slightly larger uncertainties in the calculated structural parameters of the HOPG were obtained as compared

Table 2. Critical coverage for K/graphite condensation.

θ_c	T (K)	Method	Signature	References
0.1	90	LEED	Diffraction ring stops moving and (2 × 2) appears	[18]
0.1	90	EELS	Plasmon mode stops shifting	[18]
0.35	85	Work function	Kink in $\Delta\phi$ versus θ	[5]
0.30	85	HREELS	I max of 17 meV peak	[5]
0.25	85	LEED	Appearance of (2 × 2) structure	[5]
0.3–0.4	160	UPS	Appearance of K band	[5]
0.30	90	PD exp.	Max PD yield	[28]
0.12	90	HR-LEED	Appearance of (2 × 2) structure	[10]
>0.25	??	*Ab initio* slab calc.	'Ionic-like' charge density profile	[29]
0.25	90	HREELS	Levelling of surface plasmon energy	[30]

to the SCG results. This is attributed to the randomness of the crystallites composing the HOPG sample.

4. The surface structures formed by alkali metals adsorbed on graphite

4.1. Potassium on graphite

The surface structure of K on graphite has been studied the most of any of the alkali metals on graphite. Initially, the adsorption of alkali metals on graphite was thought of as simply the first stage in the intercalation process. The first study of the surface structures of K on graphite was motivated by questions about the intercalation process [17, 24]. For all coverages, K readily intercalates into the graphite (0001) surface at substrate temperatures of 193 K and above [17, 26].

When the graphite substrate is held at liquid nitrogen temperatures ($T \cong 90$ K), at the lowest coverages ($\theta < 0.1$ ML), there is a dispersed K phase with a giant K–K spacing (up to 60 Å), indicating a repulsive K–K interaction [8, 18, 20]. Density functional theory calculations show that the K adatoms are located at the sixfold-hollow site [27, 54]. At these low coverages, rings are observed in the LEED pattern for both SCG and HOPG [8, 18, 20], indicating that the K adatoms have a well-defined nearest-neighbour spacing but no long-range orientational order. As the adatom density increases, the K–K spacing in the dispersed phase is continuously compressed until a critical coverage θ_c is reached [18]; for $\theta < \theta_c$, the dispersed or fluid phase of K/graphite has K–K spacing between 14 and 60 Å [10].

At the critical coverage, a close-packed (2 × 2) phase begins to grow until it covers the entire surface while the dispersed phase remains at a constant K–K spacing [18] with a coverage equivalent to a '7 × 7' K overlayer [10]. At higher coverages, the close-packed phase coexists with the dispersed phase—the dispersed phase remains unchanged in density and the surface area covered by the close-packed islands increases [18, 27, 10]. Different studies and different methods disagree somewhat as to the critical coverage, with most coming in at $\theta_c \cong 0.3$. Table 2 gives the various critical coverages, as well as how they were determined.

Eventually, the p(2 × 2) structure covers the entire surface, and this is defined as $\theta = 1$ ML. The K–K spacing in this structure is 4.92 Å; a top view showing the graphite basal plane and K adlayer (and associated unit cells) is shown in figure 4.

The K adatoms sit in the hollow sites of the graphite layer with a K–graphite average perpendicular spacing of 2.79 ± 0.03 Å, corresponding to an average C–K distance of 3.13 ± 0.03 Å [21]. The spacing between graphite planes is consistent with the bulk spacing of 3.35 Å [21].

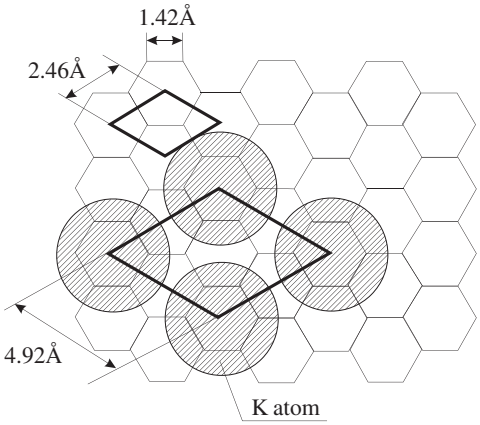

Figure 4. A schematic diagram of the (2 × 2) structure formed by K on the graphite surface. Both the substrate and the overlayer unit cells are represented.

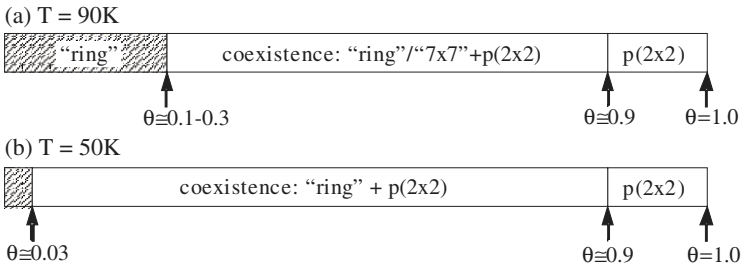

Figure 5. Equilibrium phases as a function of coverage for K/graphite [10, 15].

At surface temperatures lower than 90 K, (2 × 2) islands are seen starting at a significantly lower coverage of $\theta = 0.03$ ML [10]. Additionally, ring phases with lattice vectors between that of the '7 × 7' phase and the (2 × 2) phase are seen at $T = 50$ and 30 K; these have higher density than the '7 × 7' phase and may be explained by a local minimum in the phase diagram and reduced mobility of the K adatoms at lower surface temperatures [10]. The K/graphite phase diagram for temperatures of (a) 90 K and (b) 50 K is summarized in schematic form in figure 5.

When K is dosed on the 90 K graphite substrate above 1 ML coverage, some groups observe a $(\sqrt{3} \times \sqrt{3})$R30° structure [24, 8, 5], while other do not [18, 20]. It should perhaps be noted that the early studies showing a $(\sqrt{3} \times \sqrt{3})$R30° structure on SCG had moderately high oxygen contamination [17, 24], and that the other observations of the $(\sqrt{3} \times \sqrt{3})$R30° structure occurred on HOPG. Studies showing the (2 × 2) structure as the high-density single layer occurred on both SCG [20, 16] and HOPG [18, 20, 16]. After completion of the (2 × 2) layer, Li *et al* observe the growth of a disordered film [18, 11]. The multilayer film is stable against intercalation up to $T \approx 150$ K, above which intercalation takes place over a period of approximately 1 h [11]. The dispersed phase and the coexistence region, in contrast, intercalates at substrate temperatures as low as $T = 50$ K [11]. The surprising result that more coverage actually inhibits intercalation is interpreted as due to greater mobility in fluid phase [11].

In 2003, studies of photoemission from atomic layer resolved quantum well states (QWS) briefly revived the controversy about intercalation of monolayer K/graphite (HOPG), by claiming that the first condensed phase for $T < 100$ K is actually an intercalated (2×2) monolayer and that an adsorbed monolayer or thicker films can be grown nearly layer by layer on top of this structure [22]. A subsequent study of Na, K, Rb and Cs on graphite suggested that the observed peak was actually characteristic of a (2×2) adlayer [31] and a detailed dynamical LEED study on SCG and HOPG in the temperature range 50–140 K also concluded that the K adatoms in the (2×2) structure sit in the hollow sites of graphite on top of the surface for all cases [21].

4.2. Rubidium on graphite

Minimal work has been done on Rb/graphite, especially compared to the high number of studies on K.

Rb has been shown to form a dilute phase at low coverages, and above a critical coverage Rb condenses into p(2×2) islands, similar to K/graphite [16]. As for K/graphite, the Rb nearest-neighbour spacing in this phase is 4.92 Å, compared to 4.84 Å for metallic Rb [15]; the atomic radius of Rb makes this atom fit especially well to the graphene mesh [31]. No higher-density phases were observed for Rb/graphite [16], although a second layer only (no multilayers) could be formed for a substrate temperature of 80 K [15].

4.3. Caesium on graphite

Cs on graphite is somewhat controversial. While there is general agreement that low-coverage Cs/graphite forms a disordered 'ring' phase and higher-coverage Cs/graphite forms a rotated hexagonal incommensurate (RHI) phase, leading into a p(2×2) phase [26, 14, 16, 32], there are still questions about what happens at coverages intermediate between the 'ring' and RHI phases and coverage above that of the (2×2) phase. This makes it difficult to assign a coverage/density equal to 1 ML.

Hu *et al*, in a careful LEED study of Cs/graphite, found six superstructures: disordered, $(\sqrt{7} \times \sqrt{7})$R19°, a rotated incommensurate hexagonal phase near the (2×2) coverage, denoted as $(2 \times 2)^*$, a p(2×2), a $(\sqrt{3} \times \sqrt{3})$R30°, and a metallic + disordered phase [14]. Their phase diagram is given in figure 6; note that the coverage is defined as the ratio of adatoms to surface carbon atoms (in this scheme, a perfect p(2×2) would have a coverage of $\theta = 1/8 = 0.125$).

In the low-coverage limit, a ring structure is seen in the LEED pattern, showing that the disordered phase has a well-defined nearest-neighbour spacing, though no orientation with respect to the graphite substrate [14, 16]. This structure probably consists of large (>100 Å) regions of Cs atoms in a hexagonal array (close-packed) and indicates that in this region repulsive forces between the Cs adatoms dominate [14]. As more Cs is added, the rings get larger, indicating that the Cs structure is compressing [14, 16].

In the limited temperature range of 80–180 K, around $\theta = 0.07$ ML (1 ML here is defined as the same number of adatoms as C surface atoms), Hu *et al* observe a $(\sqrt{7} \times \sqrt{7})$R19° structure with a Cs nearest-neighbour distance of 6.5 Å [14]. This phase was not seen at all in a subsequent study of Cs/graphite [16], although a third group did see a LEED diffraction peak consistent with a $(\sqrt{7} \times \sqrt{7})$R19° structure at $\theta = 0.07$ ML on an HOPG substrate [32]. At higher coverage ($\widetilde{=}0.1$ ML) Hunt *et al* observe the $(\sqrt{7} \times \sqrt{7})$ phase to coexist with a (2×2)-*like* phase (figure 7), pointing out that the lattice parameter of the $(2 \times 2)^*$ is very similar to that of the (2×2), making it difficult to distinguish the two phases in LEED work on HOPG [32].

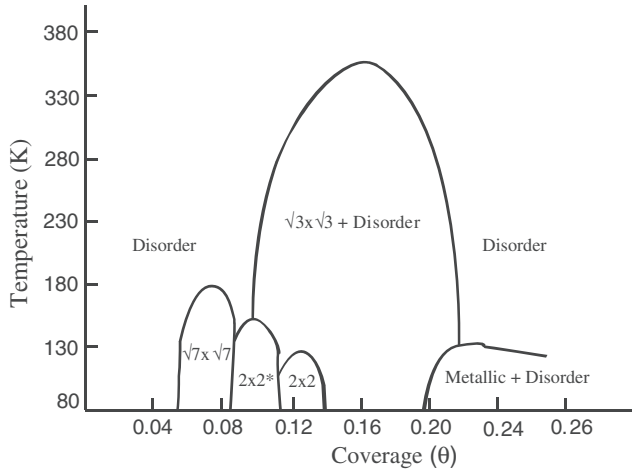

Figure 6. Phase diagram for Cs on graphite [14].

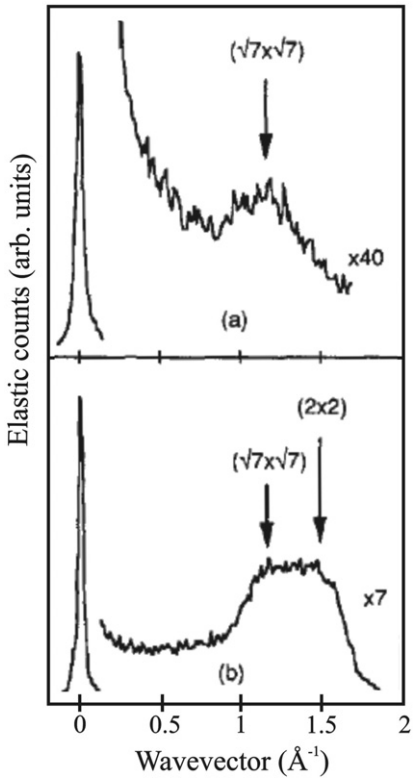

Figure 7. High-resolution LEED profiles of (a) the $(\sqrt{7} \times \sqrt{7})$ phase of Cs on graphite, corresponding to a coverage of $\theta \approx 0.13$ ML, and (b) coexisting $(\sqrt{7} \times \sqrt{7})$ and (2×2)-like phases at a coverage of $\theta \approx 0.19$ ML [32].

With the sample held at 80 K, $0.08 < \theta < 0.11$, there is a rotated hexagonal incommensurate (RHI) phase with orientational ordering. Since this phase has a lattice parameter very near that of the (2×2) phase, Hu *et al* denote this as $(2 \times 2)^*$ [14]. The orientational order of this phase fits well to a Novaco–McTague (NM) model [33], as long as the ratio of the longitudinal to the transverse sound velocity (C_L/C_T) is adjusted to 1.63, instead of the Cauchy value of 1.73 ($=\sqrt{3}$) (figure 8) [15, 34]. Above $T = 150$ K, Hu *et al* find that this phase irreversibly transforms into the $(\sqrt{3} \times \sqrt{3})$R30° one [14].

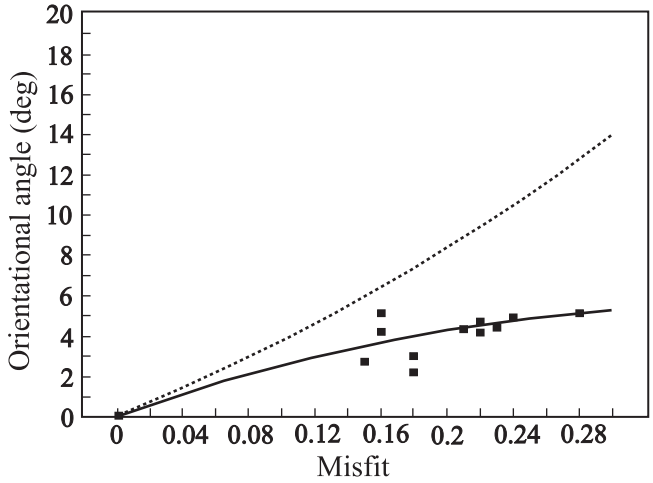

Figure 8. Epitaxial rotation angle for the hexagonal incommensurate phase of Cs/graphite as a function of lattice misfit relative to the (2 × 2) structure. The solid curve indicates the NM prediction with $C_L/C_T = 1.63$ and the dotted curve indicates the Cauchy value of $C_L/C_T = \sqrt{3}$. The experimental data are shown as black squares [15].

In the limited temperature range of 80–120 K, with $\theta \sim 0.1$, Hu *et al* see the (2 × 2) phase [14]. In this phase, the Cs adatoms are located in high-symmetry graphite locations with a nearest-neighbour spacing of 4.92 Å, about 4% smaller than the metallic Cs nearest-neighbour distance of 5.24 Å [13, 14]. LEED $I(E)$ calculations show that the Cs adatoms sit in the hollow sites of the graphite surface, 2.8 Å above the unrelaxed graphite basal plane, giving the Cs an effective radius of 2.41 Å, smaller than the metallic radius of Cs [13, 15]. This (2 × 2) phase is considered to be a full monolayer by White *et al* [16, 20], although according to Hu *et al* this phase also irreversibly transforms into the $(\sqrt{3} \times \sqrt{3})$R30° above $T = 150$ K [14].

Hu *et al* claim that the $(\sqrt{3}\times\sqrt{3})$R30° phase is the most stable of all seen, occurring at substrate temperatures between 80 and 350 K, and at coverages of $\theta = 0.1$–0.22 [14]. This phase has nearest-neighbour spacing of 4.26 Å, about 19% smaller than the metallic Cs n–n distance of 5.24 Å, but larger than the ionic Cs n–n distance of 3.38 Å [14]. This compression indicates a large charge transfer from the Cs adatom to the graphite surface [14]. The $(\sqrt{3} \times \sqrt{3})$R30° phase was not seen at all in a subsequent study of Cs/graphite, although a $(\sqrt{3} \times \sqrt{3})$R30° phase was seen when the p(2 × 2) phase was dosed with air [16]. Since the Cs compression for this $(\sqrt{3} \times \sqrt{3})$R30° phase is much larger than usually occurs on metal substrates, as well as the unusual A–A stacking of the graphite layers, White interprets this as intercalation or co-adsorption [16]. Later papers report photoemission [31] and EELS [30] from the (2 × 2) structure of Cs/HOPG without explicitly mentioning whether they consider this to be the saturated monolayer. It should be noted that while Gleeson *et al* use a definition of $\theta_{Cs} = 1$ ML at a density of 3.8×10^{14} Cs cm^{-2}, they do not actually make any claims about the coverage or structure of the highest-density overlayer [30]. Their ML definition is fixed as the density of the Cs(110) surface [35] and corresponds to one Cs adatom per five unit cells of graphite, which is 20% less coverage than the (2 × 2) phase. For the rest of this paper, we will consider that 1 ML of Cs/graphite corresponds to the (2 × 2) phase, in accordance with White [16].

With coverages clearly above one layer of Cs, the $(\sqrt{3} \times \sqrt{3})$R30° phase disordered and disappeared [14]. If left overnight, the surface transformed into a bcc overlayer of Cs on graphite with a lattice parameter of 5.8 ± 0.2 Å, compared to 6.045 Å for bcc Cs [14].

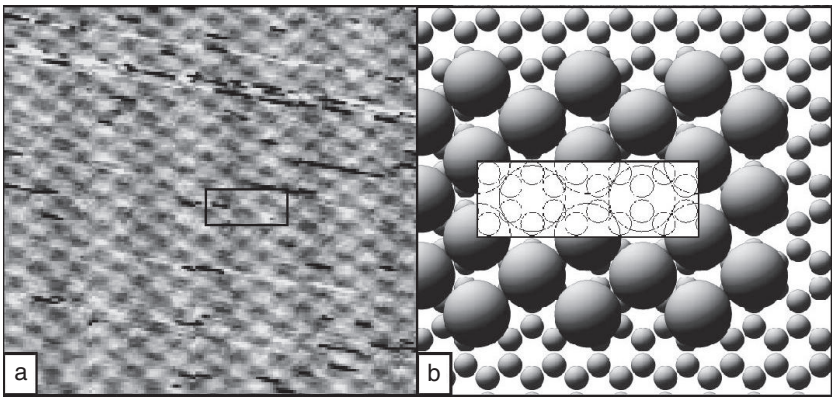

Figure 9. (a) STM image of buckled Na terrace with atoms resolved for film ∼5 ML thick at a temperature of 40 K. The image covers a 6 nm × 6 nm area. (b) The Na (110) plane overlaid on a grapheme layer (small balls). The inset shows the underlying graphene through the Na circles [37].

4.4. Lithium on graphite

No ordered or superstructure phases were found for Li/graphite for coverages between 0.1 ML and 5 ML, when the surface was held at liquid nitrogen temperatures [36, 26, 16]. Complicating matters, Li readily intercalates into graphite even at 100 K [26, 16].

After a multilayer Li/graphite crystal was annealed to 200 °C and cooled to liquid nitrogen temperatures, one group did see a ring structure in the LEED pattern [36]. AES measurements and LEED $I(E)$ curves identified this structure as small islands of hexagonal close-packed (hcp) Li (at least 100 Å) on top of the graphite surface in an incommensurate fashion with random orientation; the Li–Li nearest-neighbour distance is 3.3 Å at 80 K, which is a 6% expansion from that of metallic Li [36].

4.5. Sodium on graphite

Johnson *et al* [26] point out from their reference [8] (Asher and Wilson 1958 *Nature* **181** 409), that Na is unique among the alkali metals in that it does not readily form stage 1 intercalation compounds with graphite, but only eighth stage compounds. On both SCG and HOPG, no ordered overlayer with ∼1 ML of Na was observed, but only slightly diffuse first-order graphite LEED spots [26].

Later studies found that Na/graphite could be investigated by means of photoemission from metal quantum well states (QWSs) [37, 38]. On evaporating the Na from a glass ampoule held at a constant temperature, it was found that, from 1 to 15 ML, Na grows in a layer-by-layer fashion, although the anneal had an upper limit of 90 K [37].

At substrate temperatures of less than 90 K, Na formed monolayer islands on the graphite surface for coverages above the critical coverage $\theta_c = 0.2$ ML [38]. At substrate temperatures of 110 K, the Na underwent three-dimensional growth, in that it formed islands already 3 ML thick [38]. Atomic-resolution STM images showed these islands to be Na(110) microcrystals on the graphite surface, but with slightly buckled surfaces to accommodate the mismatch with the graphite substrate (figure 9) [37]. Note that 1 ML is defined as a full Na layer with five C atoms per Na atom, which would have a density of 7.6×10^{14} Na cm^{-2} [38]. For the rest of this paper, we will consider that 1 ML of Na/graphite has five C atoms per Na atom.

The island growth is strongly dependent on temperature. At 40 K, a disordered film grows, at 90 K there are 2 ML thick regions before the full monolayer is completed, and at 110 K the first islands, which coexist with either bare graphite regions or regions of the dispersed Na phase, are 3 ML thick [38]. A density functional theory study confirmed that small clusters of Na were energetically favourable, similar to the islands seen experimentally [39].

5. The determination of the alkali metal–graphite charge transfer. The nature of alkali metal–graphite bonding

Ideally, the complete understanding of an adsorption system would imply knowledge about the electronic interaction of the atoms involved, the position of the adatoms on the surface and the ability to predict the symmetry of the overlayer as a function of adatom coverage. As the last objective is nearly impossible to fulfil due to the many variables during the deposition/stabilization process, in the case of alkali metals on graphite the effort is channelled towards explaining the electronic interaction between the adsorbed atoms and the graphite substrate, with the more modest expectation of explaining the occurrence of certain adsorption phases once these are obtained experimentally.

The most intensive investigation of the electronic states of both adsorbate and substrate has been performed on the K/graphite system, while less information can be found in literature about other alkali metals (such as Li, Na, Rb, Cs) adsorbed on graphite. Nevertheless, similar problems are encountered in the study of all alkali metal/graphite systems, and the same experimental techniques and calculation methods are applied to solve them. Therefore, the K/graphite system will be discussed more in detail while results pertaining to the other alkali metals will be cited at the appropriate places.

The K atom has its 19 electrons arranged in the electronic configuration that can be described as argon's configuration plus an additional electron on the 4s level. The effect of bringing more K atoms together is to broaden the 4s state which becomes partly occupied.

The atomic orbitals of one C atom, in the presence of the neighbouring C atoms which make up the graphite, hybridize such that the 2s, $2p_x$ and $2p_y$ orbitals form three sp^2-type orbitals. The $2p_z$ orbital with an orientation perpendicular to the graphene layer will remain essentially unhybridized with adjacent layers. In this way, each C atom makes three σ bonds with its three nearest neighbours, and covalent π bonds (due to the $2p_z$ orbitals) with close-by atoms. In the case of two-dimensional graphite (the graphene layer), two π bands are formed: a bonding π band, fully occupied with electrons, and an anti-bonding π^* band, empty. Similarly, six σ bands are formed, of which three are bonding and three are anti-bonding (σ^*) [40]. Because the π bands are energetically closer to the Fermi level than the σ bands, they contribute significantly more to the properties of solid graphite, and thus represent the electronic bands used to describe the transport properties of the material. In making the transition between two-dimensional and three-dimensional graphite, the number of σ and π bands increases, with, again, the π bands being closer to the Fermi level. The main difference, though, is the overlap between the π bands at Fermi level in the three-dimensional case (due to a weak, but still non-zero, interlayer interaction), as opposed to a zero density of states at Fermi level for the two-dimensional graphite. This difference marks the distinction between the semimetallic properties of the three-dimensional graphite and the zero-gap semiconductor features of the two-dimensional graphite [40].

Upon adsorption on graphite, the electronic states of both K and substrate are altered as a result of charge transfer between the two types of atoms. The common-sense expectation is a transfer of charge from K towards the graphite, which modifies the occupation of the K 4s orbital as well as the position of the graphite Fermi level due to the addition of carriers to

the bulk material. The problem that arises then is twofold: which graphite bands is the charge transferred to, and how much charge is transferred from the adatoms to the substrate. The answer to the latter question would elucidate the character of the K–graphite bond: an ionic bond would imply a K 4s resonance state narrow and empty, situated above the Fermi level, as opposed to a covalent bond where the 4s resonance spreads across the Fermi level, half-filled [50]. Evidently, any incomplete charge transfer would mean an intermediate situation between the two extreme ones just mentioned. In addition, there is always the possibility that the adsorbed atoms 'share' their electrons rather than transfer them to the substrate, which would result in a charge smearing within the adlayer, translating into a metallic character of the adsorbate. The shift between specific electronic interactions is induced by the density of adsorbed atoms, thus the nature of the bonding is expected to change with coverage.

The tasks at hand, therefore, are to determine the density of states (DOS) at Fermi level, to judge the individual contribution of various electronic states to this DOS, to calculate the shift in the graphite's Fermi level and, ultimately, to convert the accumulated information into a quantitative estimation of the electronic charge transfer between adatoms and substrate; and to do all this as a function of adsorbate coverage. Usually, this course of action describes the pure theoretical approach: first-principles calculations which resolve the bonding properties of adsorbed alkali metal atoms on graphite. There are, nevertheless, alternative methods to the steps enumerated above. These imply an indirect experimental determination of charge transfer—a procedure that starts with experimental data which, upon computational manipulations, provide the hoped for information.

5.1. Calculation of alkali metal–graphite charge transfer having experimental data as starting point

Several experimental techniques have been successfully applied in the study of alkali metal/graphite adsorption systems. As a result, knowledge about the change of the work function, the magnitude of the induced dipole moment at the position of the adsorbed atoms, the shift in position of the substrate's Fermi level due to adsorbed atoms, and the corrugation of the surface potential, to mention just a few, has been gathered upon investigating the interaction of electrons, photons or atoms with the systems under study. Still, it is necessary to translate the experimental data into parameters that would explain and quantify the adsorbate–substrate electronic interaction; therefore, a certain manipulation of the data is required based on theoretical arguments. The current section intends to briefly summarize some of the experimental techniques, the calculations involved, and their relevant end product—be it numerical values or explanations for experimentally observed features. Although precise values have been quoted from the articles in question (e.g. for the amount of charge transferred between adsorbate and graphite, for the induced dipole moment, etc), in most cases the authors recognize a certain level in the uncertainty of these values: not only are the experimental data affected by typical errors, but their consequent use in calculations is subject to the assumptions characteristic to each theoretical method, some assumptions being simplifying hypotheses, others just a reflection of the limited knowledge in the domain.

5.1.1. Surface investigation by electron spectroscopy. Electron energy loss spectroscopy (EELS), sometimes referred to as high-resolution electron energy loss spectroscopy (HREELS), a distinction made mainly based on the energy of the incident electrons probing the sample, has been repeatedly used in the study of graphite/alkali metal systems. At primary electron energies less than 20 eV, HREELS essentially probes the surface of a sample. It analyses inelastically scattered electrons which leave the surface with an energy differing from

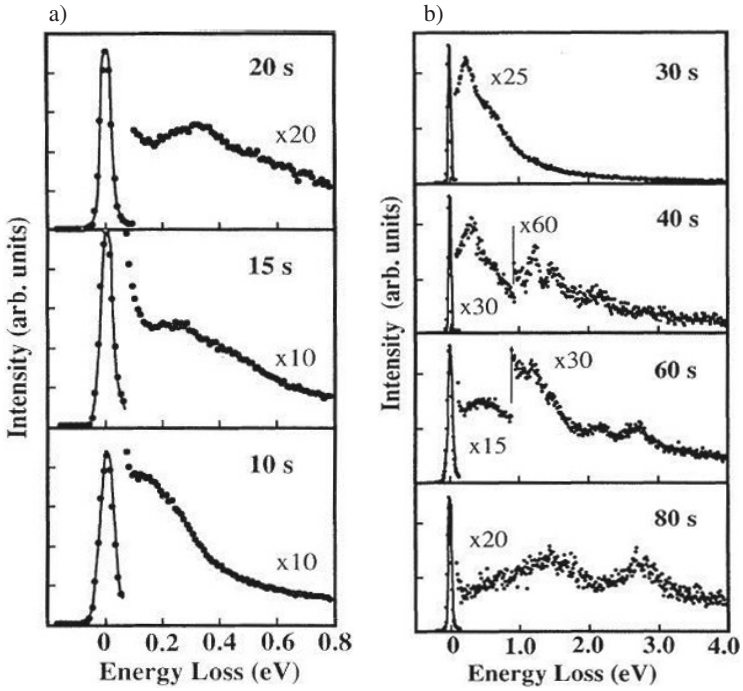

Figure 10. HREELS spectra for K adsorbed on graphite obtained by Li *et al* [18]. The coverage is inferred from the evaporation time. Panel (a): at low coverage, the plasmon peak shifts towards higher energy with increasing coverage, and reaches a maximum value of ≈320 meV at a critical coverage. Panel (b): at higher coverage, the plasmon peak is replaced by three loss peaks at 1.2, 1.5 and 2.2 eV, which are ultimately replaced by a 2.7 eV surface plasmon attributed to bulk K.

the primary energy by an amount characteristic of a phonon, a plasmon, or the vibration of an adsorbed atom. The experimental data are in the form of intensity of the outgoing electron beam versus its change in energy, i.e. in the form of a loss spectrum.

EELS in combination with high-resolution low-energy electron diffraction has been used by Li *et al* [18, 41] to investigate K adsorbed on graphite as a function of coverage. The temperature of the system was kept at 90 K in order to avoid intercalation. For K coverages less than 0.1 ML, the EELS spectra display a plasmon peak that shifts with increasing coverage from about 50 to 320 meV and subsequently dies away as more K atoms are adsorbed. Concomitant with the disappearance of the plasmon mode, three other loss peaks, at 1.2, 1.5 and 2.2 eV, appear, marking a qualitative change in the system. Indeed, the coverage at which the plasmon mode ceases to shift and starts fading away corresponds to the transition from K-dispersed phase to the formation of close-packed, (2×2) islands, information extracted from the LEED profiles. Figure 10(a) shows a sequence of EELS spectra corresponding to low K coverage, illustrating the shift in energy of the plasmon peak, while figure 10(b) shows similar spectra at higher coverage, where the three loss peaks replace the plasmon mode.

The plasma mode is attributed to the graphite substrate and its shift is assigned to an increase in graphite's charge carriers due to a redistribution of charges from K towards the substrate. Evidently, with increasing K coverage, more charge is transferred to graphite and this determines the peak's shift. The fading away of the plasma mode once the (2×2) islands start forming can be explained by another type of charge redistribution: instead of charge being somewhat transferred to the substrate, the redistribution takes place within the K adlayer,

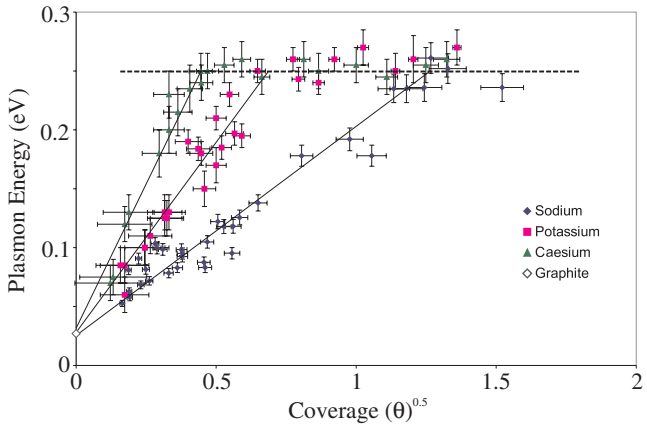

Figure 11. Energy of the plasmon excitations obtained by EELS for Na, K and Cs adsorbed on graphite, as a function of the square root of the alkali coverage (from [30]). The plasmon mode levels off at the same energy (approximately 250 meV) for all three adsorption systems, as the coverage reaches a critical value corresponding to the transition from dispersed to condensed phase.

(This figure is in colour only in the electronic version)

sustaining the idea of a metallic character of the adsorbate. The three loss peaks are attributed to transitions between the 4s and 4p bands of two-dimensional K. As the coverage increases beyond one monolayer, the features characteristic to the condensed phase are replaced by a broader loss peak at 2.7 eV, attributed to a metallic K surface plasmon previously observed in EELS studies of solid K [42]. This peak at 2.7 eV is already evident in the high-coverage spectra shown in figure 10(b). By applying band structure calculations [43] for the K–graphite dispersed phase, the change in plasmon mode frequency can be related to a shift in the Fermi level of graphite (since the interpretation of charge transferred towards graphite is consistent with the idea of an upward shift of the Fermi level). Ultimately, the position of the Fermi level is quantitatively related to the number of charge carriers added to the bulk material, according to the results of Tatar and Rabii [44]. Assuming that charge is mainly transferred to the topmost graphite layer, a value of $0.7e$ is calculated for the charge transferred per K atom, at coverages less than 0.1 ML [18, 41].

Similar EELS experiments (with an initial electron energy of 25 eV) have recently been performed on adsorption systems involving K, Cs and Na dosed on graphite at low temperature (89 K) and at low coverage [30]. In accordance with earlier studies [18, 41] the plasmon energy is found to shift towards higher values as the coverage increases and eventually levels off at the coverage corresponding to the transition from the dispersed to the condensed phase. This particular coverage is 0.25 for K and 0.2 for Cs, and 1.45 for Na—an exception in the sense that Na forms clusters even at low coverage. It is interesting to note that the energy at which the plasmon mode levels off is the same for all three types of alkali metals: approximately 250 meV (see figure 11). No explanation is yet provided for this behaviour. Calculations of the predicted plasma frequency based on the free electron model [45] indicate a linear dependence of the plasmon energy, $\hbar\omega$, on the square root of the coverage, $\sqrt{\theta}$. This predicted linear dependence is confirmed by the experimental EELS data: plots of the Na-, K- and Cs-induced plasmon losses versus the square root of the coverage are shown in figure 11. From the initial slope of the plots, it is possible to calculate the charge transferred from the alkali metal to graphite at low coverage: 0.1–0.2e, 04–0.5e and 0.6–0.8e per atom for Na, K, and Cs, respectively.

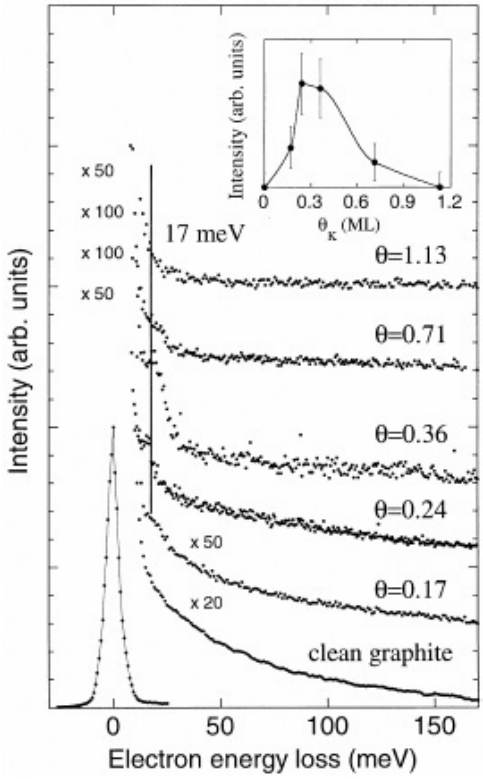

Figure 12. HREELS spectra obtained by Österlund *et al* [5], for clean graphite and K adsorbed on graphite at different coverages. A loss peak at about 17 meV appears at a K coverage of 0.17, reaches a maximum in intensity for $\theta \approx 0.3$, and eventually disappears as the coverage reaches 1 ML. Inset: the intensity of the loss peak as a function of coverage.

The same technique has been applied by Österlund *et al* [5] using a much lower energy of the incident electrons: 1.5 eV. The HREELS spectra shown in figure 12 feature a well-resolved loss peak at about 17 meV which appears at a K coverage of 0.17, reaches a maximum in intensity for $\theta \approx 0.3$, and eventually disappears as the coverage reaches 1 ML.

The peak can be assigned to the vibration in a direction perpendicular to the surface of the K atoms in the dispersed phase. According to the dipole scattering theory [46], the charge associated with the vibrating K atom can be estimated by a fitting procedure: its value is changed till the experimental loss intensity at 17 meV is reproduced in calculations. The charge thus obtained equals, in the point charge approximation, the amount that one K atom transfers to the substrate: $0.38 \pm 0.11e$. The dipole moment obtained from combining the value of charge transferred with a 2.68 Å distance from the K atom to the graphite plane is approximately $11.9D$, while a K–C distance of 3.53 Å gives $9.8D$. The fact that the position of the loss peak does not shift with coverage in the range $0.17 < \theta < 0.36$ indicates that in the dispersed phase the K–K distance remains constant, ensuring an unchanged local environment of the K atoms. As the coverage increases, the loss spectrum resembles the continuum loss spectrum observed for metal surfaces, indicative of the metallic character of the K adlayer at $\theta \geqslant 1$.

5.1.2. Work function change measured by UPS and the RP method. Another approach to obtaining a value for the transferred charge between K and the graphite substrate is to calculate it from the variation of the work function, $\Delta\Phi$, as a function of K coverage. In the case of low coverage, $\Delta\Phi$ varies directly proportionally with the number of adsorbed atoms per unit area,

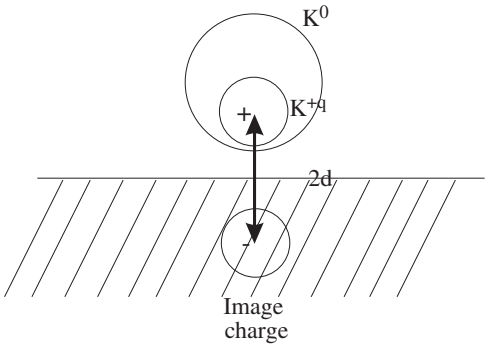

Figure 13. The interpretation of the dipole in the image charge model: the ends of the dipole are located at the centre of the K^{+q} ion and its image charge in the substrate. Upon transferring charge to the substrate, the neutral K atom (K^0) reduces its size to a value corresponding to the ionic K (K^{+q}).

N_a, and the surface dipole moment per adatom, μ, according to the Helmholtz relation [47]:

$$\Delta\Phi = -2\pi e N_a \cdot \mu(\theta). \tag{1}$$

The dipole moment is then obtained from the slope of $\Delta\Phi$ versus coverage:

$$\mu(\Phi) = -\frac{1}{2\pi e}\left[\frac{\mathrm{d}(\Delta\Phi)}{\mathrm{d}N_a}\right]. \tag{2}$$

As illustrated in figure 13, using an estimated distance d which comes close to the K–graphite bond length enables one to calculate the charge transferred at each adsorbate site:

$$q = \frac{\mu}{2d} = -\frac{1}{4\pi e d}\left[\frac{\mathrm{d}(\Delta\Phi)}{\mathrm{d}N_a}\right]. \tag{3}$$

Equations (1)–(3) have been applied to the change in work function versus coverage data obtained by either the retarding potential (RP) method or ultraviolet photoemission spectroscopy (UPS) in the submonolayer regime of K adsorbed on graphite [5, 8]. Figure 14 shows the change in work function, from a 4.7 eV value (the graphite work function [48]) to a 2.3 eV value (the work function of a 5 ML K on graphite), as a function of K coverage.

The experimental data give a value of $0.5e$ for the charge transferred per K atom, in the low-coverage regime as reported be Hellsing *et al* [8], or a slightly lower value of $0.37 \pm 0.05e$ for coverage below 0.3 obtained by Österlund *et al* [5]. In both cases, d was estimated to 2.68 Å, a value that compares well to the equilibrium K–graphite bond length in the case of $\theta = 0.25$. The dipole moment induced at the position of one K atom can be calculated from the linear part of the graph ($\theta < 0.15$), and yields a value of 9.4 ± 1.5 D [5]. Additional features in the $\Delta\Phi$ versus θ plot, such as the absence of a minimum (which would be expected if the substrate was a metal or semiconductor), and the change in slope (a levelling of the curve) at a well-defined coverage, support the main feature of the K/graphite adsorption systems: the existence of a critical coverage θ_c. For coverages below θ_c an increasing amount of charge is transferred from K to graphite with increasing coverage. Above θ_c the charge is shared by the K atoms producing a metallic behaviour of the adlayer. This is the same critical coverage seen in the structural studies: the point where the condensed phase begins to grow while the dispersed phase remains at a constant nearest-neighbour spacing.

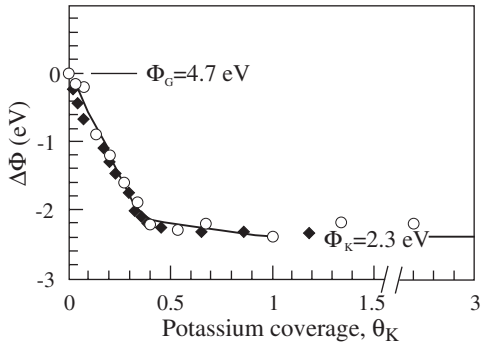

Figure 14. The change in work function versus K coverage measured by Österlund *et al* [5] using two different techniques: the RP method (○) and UPS (◆). The graph does not exhibit a minimum in the submonolayer regime as expected for alkali metal adsorption on metal and semiconductor surfaces.

5.1.3. Electronic states probed by photoemission and photoabsorption spectroscopy. The condensed (2×2) structure formed by both Cs and K on graphite has been the subject of an x-ray photoelectron spectroscopy (XPS) study by Johnson *et al* [26], with a different conclusion about the charge transfer assumed to take place between the alkali metal and the substrate. In XPS, electrons expelled by photons from distinct core levels belonging to the adsorbed species leave the sample with a certain kinetic energy which is related to their binding energy. The experimental data consist of a series of energy distribution curves: the intensity of the emitted photoelectron beam versus binding energy, for various directions of emission. The features of the experimental spectra are usually reduced to a diagram plotting the initial-state binding energy versus the component of momentum parallel to the surface. According to the data of Johnson *et al* [26], the comparison of the calculated valence and conduction band of clean graphite [44] with the binding energy diagram of Cs in the (2×2) structure indicated that a shift of 1.7 eV in the position of the theoretical graphite bands was necessary for a good fit. This shift was attributed to the charge transferred from Cs to the graphite layer. Assuming the charge to be transferred into the substrate π^* band, its value, calculated using the results of Tatar and Rabii [44], amounted to $0.9 \pm 0.1e$ per Cs atom [26]. A similar result was reported for K adsorbed on graphite in the condensed phase, one of the few studies to report a complete charge transfer in the case of ordered (2×2) K overlayers (see also [49, 55]). Based on the similarity of the spectra of K intercalated into graphite with the spectra of the (2×2) K overlayer, it was concluded that the charge transfer remained close to $1e$ per K atom even for intercalation compounds. In the same study [26], XPS measurements of Na adsorbed on graphite at an approximate coverage of 1 ML (1 ± 0.3 ML) concluded that an amount of less than $0.1e$ was transferred from Na to the substrate. The result implies that Na exists on the graphite surface in atomic form, not as ions, a feature that makes this particular element unique among alkali metals. This lack of interaction via charge transfer might explain why Na intercalation compounds do not form easily. The same study [26] applied to the Li/graphite adsorption system indicated a complete charge transfer into the graphite π^* band, for an Li coverage estimated between 1 and 3 ML. Once the deposition was over, the emission from the π^* band decreased with time and almost disappeared 80 min after evaporation, while the emission from the π and σ valence bands moved towards the Fermi level by 0.5 eV. This was interpreted as an indication of Li diffusion into the graphite. The conclusion was not surprising, since the Li atoms are small, have a large ionization potential and sufficient mobility even at low temperatures (100 K).

Photoelectron spectroscopy (PES) measurements of the C 1s and K 3p levels, as well as of the graphite valence band, were performed by Bennich *et al* [19], using photons of different energies (1487, 350, 100 and 40.8 eV), probing K adsorbed on graphite at coverages up to 1 ML. The study finds C 2p bands around the Fermi level for the dispersed phase of K/graphite, and K 4s bands for the (2×2) phase of K/graphite. This supports the picture of charge transfer from K to graphite at low coverage, and the formation of a metallic K 4s-derived band in the condensed phase, without ruling out the possibility that some charge transfer is taking place even in the (2×2) phase. The binding energy of the graphite σ and π bands, as well as of the C 1s line, shifts depending on K coverage. Using the rigid band model which assumes an adsorbate–graphite interaction based strictly on charge transfer with practically no influence upon the graphite electronic bands, it is possible to convert the binding energy shift to an estimated value of the transferred charge. The procedure involves integration of the charge in the DOS (calculated for clean graphite) upon shifting the Fermi level by an amount estimated from fitting experimental with theoretical data. The calculations assume that charge is transferred to the first two graphite layers. The results indicate a charge transfer in the range 0.15–0.18e/K atom in the saturated dispersed phase (a phase described by a (7×7) unit cell) and 0.012e/K atom in the condensed (2×2) phase. It has been suggested, though, that a higher value (0.36e instead of 0.18e) should be obtained by taking into account the spin degeneracy of the DOS used for calculating the charge transfer [38]. Breitholtz *et al* [38], making calculations along the same line, obtain a charge transfer of 0.2e per Na atom, for 0.2 ML Na adsorbed on graphite. Still, the applicability of the rigid band shift method itself is questioned based on non-negligible influence of the adsorbate upon the graphite bands [38].

The strength of experiment joining forces with calculations is illustrated by the results of XPS and XAS (x-ray absorption spectroscopy) measurements combined with first principles calculations, on the dispersed phase of K on graphite [50]. Although the measurements were performed on graphite covered with one monolayer of Ar, they were still used for the K/graphite system, based on the assumption that the valence electron distribution of Ar with a core hole is the same as the electron distribution of a K atom (the $Z + 1$ approximation). Thus, XA spectra help position the 4s resonance level of an isolated K-like Ar adatom 1.6 eV above the Fermi level. This value is confirmed, within a 0.1 eV range, by first principles calculations applied to a single K atom positioned on a graphite layer at the same distance as an argon atom would be (i.e., 3.2 Å). Although not relevant in the K/graphite case, the agreement presents the importance of validating the calculations by comparison with experiment. Next, the decay spectra of the core-ionized state (XPS) and the decay spectra of the core-excited state (XAS) serve to calculate the characteristic charge-transfer time of one 4s electron from an argon atom to the substrate and, related to it, the hybridization width of the 4s level. Using the above-mentioned experimental data and correcting the calculations for a K atom at the proper adsorption distance (2.6 Å) above the graphite layer, the 4s level of K on graphite in the dilute phase is found to be 2.7 eV above the Fermi level and 0.1 eV wide [50]. Thus, the importance of the result is twofold: not only does it provide evidence for an ionic bond of K on graphite in the dispersed phase, but it also proves the potential of applying the same experiment–calculation method for other alkali metal adsorption systems.

5.1.4. Surface potential corrugation investigated by He-scattering. Another technique that can provide information about the electronic structure of surfaces is He-scattering. The intensity of the He diffracted beam constitutes an indication of the surface potential corrugation which is, in turn, dependent on the electronic charge distribution at the surface. Therefore, it is no wonder that the technique has been applied to the study of alkali metal/graphite systems [16, 20, 51]. Somewhat surprising, though, is the negative result of the experiment: no

He diffraction was observed from graphite substrates covered with a monolayer of K, Rb or Cs. Taking into account the experimental capability of detecting diffracted intensities of the order of 0.1% of the specular intensity for a 17.4 meV He beam, the no-feature diffraction scans indicate diffraction intensities below the experimental sensitivity. In order to predict theoretically the intensity of the expected scattered He beams, a necessary step is the computation of the potential experienced by a He atom approaching a (2×2)-structured monolayer of alkali metal atoms. The outcome of the calculation is a very small potential well depth ($\leqslant$1 meV), for any of the adsorbed species on graphite. Consequently, the predicted diffraction intensities are of the order of 5% of the intensity of the specular beam, still well within the sensitivity attributed to the experiment. The small potential corrugation can be interpreted as arising from charge redistribution within the alkali layer and the formation of two-dimensional quasi-free electron bands. It is possible that accounting for such a redistribution of charge associated with the adatoms would decrease the corrugation of the calculated potential. Also, inelastic effects, associated with alkali metal vibrations, would affect the corrugation in the same direction and help resolve the inconsistency between experimental and theoretically predicted diffracted intensities.

5.2. Theoretical calculations of alkali metal–graphite charge transfer

The theoretical approach very often makes use of either one or both of the following simplifying assumptions. First, since the interaction between successive graphite planes is weak, the calculations always have a 2D graphene layer as a starting point, following that additional layers are taken occasionally into account as a perturbation. Second, the studies of single K atoms adsorbed on graphite are assumed to bring valid information about the adsorption systems in the low coverage regime, an assumption that relies on the fact that the K–graphite interaction is much stronger than the K–K one, provided that the distance between adjacent adatoms exceeds a certain value.

For the sake of simplicity, the various theoretical studies have been labelled according to the most prominent result obtained by each individual study.

5.2.1. The semimetallic character of graphite—a cause for the structural phases formed by K on graphite. The simplified tight-binding model was used by Ishida and Palmer [27] to calculate the electronic structure of K on graphite. The calculations consider one graphite layer and a variable number of K adatoms, corresponding to a coverage ranging from very low (one K atom per 800 C atoms) to approximately 1 ML (one K atom per six C ones). The various terms in the system's total energy indicate that at low coverage, following a charge transfer from K to graphite, the dipole–dipole interaction (also called the electrostatic term) is less important than the band energy term. The latter term is due to the insufficient screening of the positive charges by graphite, an explanation based on the semimetallic nature of the graphite. Had the substrate been a metal instead of a semimetal, good screening of the K ions was expected, and the dispersed phase of K would have been explained based on the predominant dipole–dipole repulsion. The difference in the substrate character might explain the way K, when adsorbed on such substrates, changes its structural phases: a smooth transition, depending on coverage, for a metallic substrate versus a non-smooth transition, such as the one from the dispersed phase to the (2×2) superstructure, for a graphite substrate.

5.2.2. Calculated electronic charge density of the K/graphite system as an illustration of the K/substrate charge transfer and the system's potential corrugation. Ancilotto and Toigo [29] report first-principles total-energy calculations applied to K adsorbed on graphite, for two

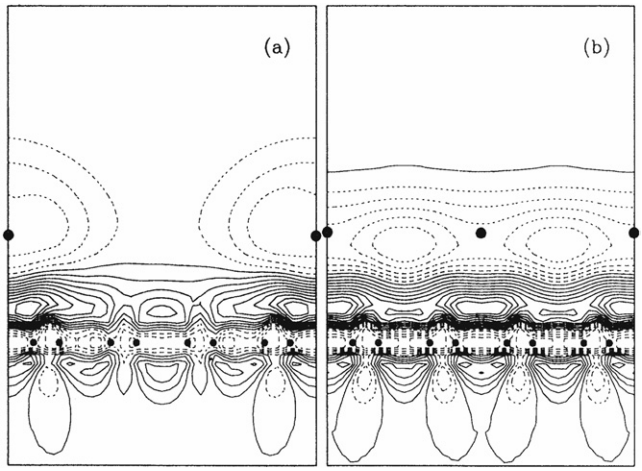

Figure 15. The difference between the electronic charge density of the K–graphite system and the combined electronic charge densities of clean graphite and isolated K monolayer, i.e. $\Delta\rho(r) = \rho_{K-C} - (\rho_K + \rho_c)$, projected onto a plane perpendicular to the K/graphite surface (from [29]). The K atoms are represented by large dots, while the small dots represent the C atoms. (a) The case of low K coverage; (b) K in the condensed, (2×2) phase.

different coverages: one corresponding to the observed (2×2) structure, and a low coverage with one K atom corresponding to 32 C atoms. The K atoms in both cases are found to adsorb in hollow sites, at a distance above the graphite plane of 2.82 and 2.77 Å, respectively. The binding energy per K atom is 0.48 eV in the (2×2) phase and 0.78 eV in the dispersed phase. Slightly different results are obtained for calculations in which the graphite monolayer is allowed to relax, an effect which is attributed, in part, to the approximations used in the calculations. The computation of the electronic charge density of the K/graphite system and how it relates to the combined electronic charge densities of clean graphite and isolated K monolayer, indicates, in the disperse K phase, a charge transfer from the K 4s orbital as well as from the graphite σ bonds towards the graphite π^* antibonding orbitals. Figure 15(a) pictures the change in electronic charge density upon adsorption of K on graphite, along the surface of the K/graphite system, supporting the above-mentioned interpretation of charge transfer. Quite similarly, figure 15(b) shows that in the (2×2) structure, charge is depleted from between the K atoms (much closer apart than in the previous coverage), which now form a quasi-metallic adlayer, and also from the C layer, and redistributes in the region between the K and graphite layers.

The calculated charge transfer from K towards graphite is $0.18e$ in the (2×2) structure and $0.38e$ in the dispersed phase, for an unrelaxed substrate. In addition, the contour plot of the charge density corresponding to the electronic state that appears close to the valence-band edge of the graphite substrate, illustrated in figure 16, suggests the existence of delocalized electrons in the (2×2) case, probably originating from the K 4s electrons. The smoothness of the contour plot is an indication of a very small surface corrugation, in agreement with the findings of He-scattering experiments [16, 20, 51] which showed no diffraction off the K/graphite surface.

5.2.3. Charge transfer as a function of coverage inferred from the calculated density of states for K on graphite. The theoretical investigation of the bonding properties of K on graphite can be further exemplified by the work of Hjortstam *et al* [52], who applied a full-potential slab

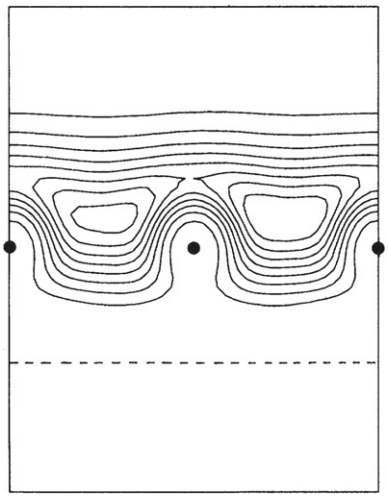

Figure 16. Contour plot of the charge density for an electronic state situated close to the valence-band edge of the graphite monolayer, introduced by the K (2 × 2) overlayer. The existence and energy position of the state has been calculated in the Kohn–Sham approximation by Ancilotto *et al* [29]. The dots represent the K adatoms, and the dashed line indicates the position of the graphite monolayer.

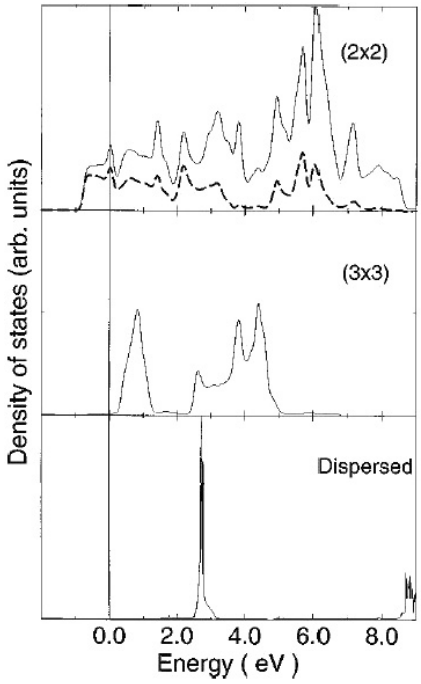

Figure 17. Calculated DOS for K on graphite at three different coverages. From top to bottom: K in the (2 × 2) structure, K in the (3 × 3) structure and K in the dispersed phase (from [52]). The vertical solid line marks the position of the Fermi level. For the (2 × 2) structure, the K 4s contribution to the DOS is shown with dashed line.

method, based on linear muffin-tin orbitals, for various K structures: a disperse phase (with a K–K distance greater than 14 Å), the hypothetical (3 × 3) structure, and the experimentally observed (2 × 2) structure. In accordance with the previous studies [27, 29], an ionic bonding is inferred for the dispersed and the (3 × 3) phase, whereas in the (2 × 2) phase the K adlayer appears to be metallic. The conclusions are derived from the calculated density of states projected on the K atoms for the three cases, with an analysis of the contribution of the K 4s state to the DOS. The calculated DOSs are shown in figure 17.

Starting with the most dilute K adlayer and moving towards the more dense structures, the 4s derived peak evolves from a narrow (0.10–0.15 eV wide) peak, situated 2.7 eV above

Table 3. The K binding energy, its equilibrium distance from the graphite surface and the charge transferred per K adatom, calculated for two different K superstructures: (2×2) and (4×4) formed on 1, 2 or 3 graphite layers [53].

System	E_{binding} (eV)	$d_{\text{K-graphite}}$ (Å)	Charge transfer
K(2×2) on 2 graphite layers	0.98	2.82	$0.17e$ ($0.11e$ to the 1st layer, and 0.05 to the 2nd)
K(4×4) on 1 graphite layer	0.44	2.82	$0.27e$
K(4×4) on 2 graphite layers	0.52	2.80	$0.40e$ ($0.16e$ to the 1st layer and $0.23e$ to the 2nd)
K(4×4) on 3 graphite layers	0.51	2.79	$0.37e$ ($0.11e$ to the 1st layer and 0.20 to the 2nd)

the Fermi level, into a feature 0.9 eV wide and approximately 1 eV above E_F, and finally into a broader band, partly occupied, that straddles the Fermi level, in the case of the (2×2) overlayer. The very narrow 4s peak obtained in the dilute K phase is an indication of the ionization of the K atoms and, consequently, implies a small hybridization between the K and the graphite states [52]. This can be explained based on the symmetry of the K 4s orbital and the C p_z orbitals. The 4s orbital, with a spatial extension that exceeds the K–graphite bond length (2.6 Å), overlaps the graphite π^* band, made up of C p_z orbitals that have a positive and a negative lobe on opposite sides of the graphite plane. An actual cancellation of the different parts of the overlap integral is expected due to the symmetry of the orbitals involved. Both the position and the width of the 4s derived peak in the disperse phase compare well with the experimental values obtained from photodesorption data [7, 8], as well as with the data obtained from XAS performed on Ar adsorbed on graphite [50]. The calculation of the cohesive energy of the K atoms gives a value of 3.88 eV in the (2×2) structure and 3.74 eV in the (3×3) one [52]. The slightly greater cohesive energy in the case of the condensed phase is attributed to a larger overlap of the K 4s orbitals in this structure as opposed to a smaller contribution of the 4s states to the chemical bond in the (3×3) structure. The fact that it is energetically more favourable for K to form a (2×2) overlayer is reflected in the experimentally observed phase transition: as the coverage increases, the K adlayer goes from a dispersed phase to the formation of (2×2)-type islands without the occurrence of the (3×3) structure which is proven to be energetically less favourable.

5.2.4. The variation of the charge transfer with the number of graphite layers considered in theoretical calculations. An illustration of how more than one graphite layer affects various parameters obtained from charge density calculations is given by Lamoen and Persson [53]. The application of first-principles methods within the density functional formalism to K adsorbed on one, two and three graphite layer substrates give comparable but nevertheless slightly different values for the binding energy per K atom, the K–graphite equilibrium distance and the amount of charge transferred from K towards the substrate. Table 3 shows the values obtained in the case of two K superstructures, (2×2) and (4×4), with the adatoms situated in hollow sites of the graphite.

5.2.5. Suggested intercalation–desorption mechanism for K on graphite. The extreme case of very low K coverage can also be studied based on individual K atoms adsorbed on C clusters. The cluster model solved within the framework of local spin density approximation (LSDA) and generalized gradient approximation (GGA) by Lou *et al* [54], reiterates the picture of a large charge transfer from K towards the substrate, which decreases as more K atoms adsorb beyond the critical coverage. The calculated dipole moment ($9.45D$) associated with the nearly ionized, singly adsorbed K atom compares well with the experimental value ($9.5\pm2.0D$) [5],

a fact that can be regarded as a confirmation of the theoretical prediction of $0.64e$ charge transfer at very low coverage [54]. The value drops to $0.54e$ per adsorbed atom as θ increases to 0.25, and to $0.46e$ for coverage that equals 1. Again, the metallic character of the K overlayer at high coverage is confirmed by a decrease in the charge transferred to the substrate due to the redistribution of electrons within the K layer. The cluster calculation also provides insightful information about the binding energy of singly adsorbed K atoms. For example, a much larger binding energy (between 1.44 and 1.65 eV, depending on the calculation method) is obtained for individually adsorbed atoms than for the case of multiple K adsorption. In addition, the binding energy of a singly adsorbed K atom varies as a function of the adsorption site, the maximum variation being between a hollow site and a bridge site. This value of approximately 0.22 eV (the diffusion energy) on the one hand, and the energy necessary to detach K atoms from the (2×2)-structured islands (an estimated 0.86 eV melting energy) on the other hand, set the range for the activation energy for intercalation, E_{interc}: $0.22\ \text{eV} < E_{\text{interc}} < 0.86\ \text{eV}$. A kinetic model, implying several stages, is presented for the intercalation–desorption process: a thermally activated surface diffusion followed by the actual intercalation at a defect site and, finally, desorption—provided the temperature of the sample increases even further. However, if K is already in the condensed phase on the graphite substrate, it is suggested that the intercalation would commence only after the adatoms space out into a disperse phase (corresponding to a melting of the (2×2) islands) [54]. This mechanism would explain the experimentally based conclusion that the condensed phase is more stable against intercalation than the dispersed phase [5, 11].

6. Conclusions

A summary of the experimental and theoretical data pertaining to the alkali metals/graphite adsorption systems proves to be very uneven: much more information is available about K on graphite than for Li, Na, Rb or Cs adsorbed on the same substrate. A brief inventory of the currently known aspects and also of the problems still left to resolve is presented below.

6.1. The surface structures formed by the alkali metals on graphite

The most striking thing about the structure of alkali metals on graphite is how similar the phase diagrams are for the larger alkalis: K, Rb and Cs (figure 18). There are several features that these particular adsorption systems share: a certain succession of phases and the existence of critical coverages that mark the transitions between phases.

At liquid nitrogen temperatures, the initial adatoms form a disordered 'ring' structure characterized by a well-defined nearest-neighbour distance and the lack of any long-range orientational order. The nearest-neighbour distance continues to compress until the ring phase saturates. Both K and Rb clearly have a critical coverage θ_c, above which the ring phase coexists with $p(2 \times 2)$ islands on the graphite surface. The islands grow and the area covered by the dispersed phase shrinks until the entire surface is covered with a (2×2) monolayer. Cs behaves in a similar fashion to K and Rb, although a rotated hexagonal incommensurate phase exists at intermediate coverages between the ring and the (2×2) phases, as well as (possibly) a $(\sqrt{7} \times \sqrt{7})\text{R}19°$ structure at lower intermediate coverages [32, 14, 34, 16].

Na, due to its smaller size, does not fill the surface in a (2×2) structure. Figure 19 shows the phases of Na/graphite. With a substrate temperature below 90 K, the initial adatoms again form a ring phase which saturates at a coverage of $\theta \cong 0.2$. Above the critical coverage, Na bcc(110) microcrystals grow and the area covered by the dispersed phase shrinks until the entire surface is covered with a buckled bcc(110) monolayer. The full Na monolayer has about 60% more adatoms than that of the larger alkalis.

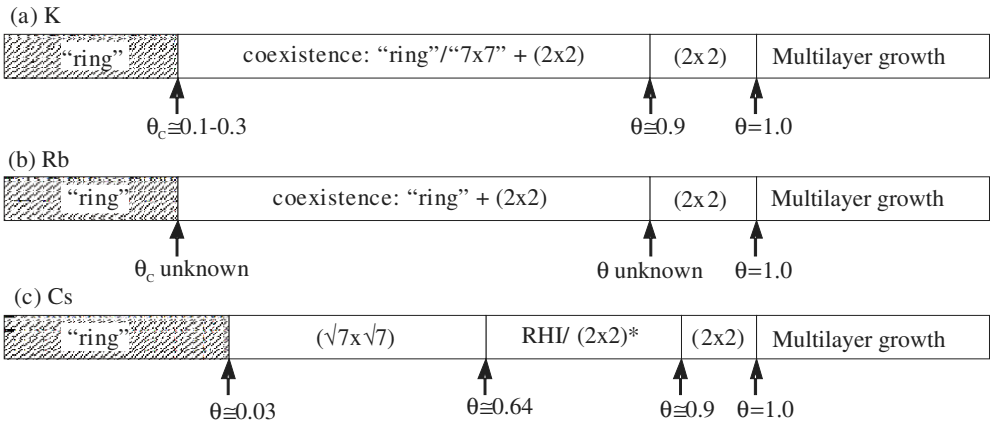

Figure 18. Equilibrium phases for $T \approx 90$–130 K as a function of coverage for larger AM/graphite, assuming after White that the $(\sqrt{3} \times \sqrt{3})$ Cs–graphite phase seen by Hu *et al* was due to contamination [10, 14–16, 32]. $\theta = 1$ ML corresponds to one adatom for every eight surface C atoms, $\rho = 4.8 \times 10^{14}$ K atoms cm^{-2}.

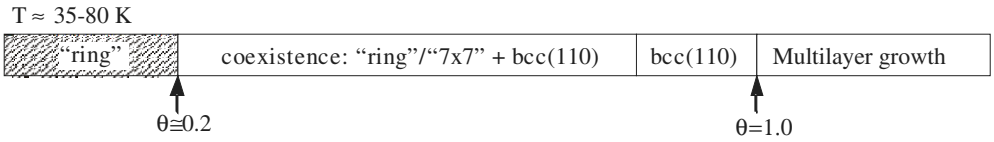

Figure 19. Equilibrium phases as a function of coverage for Na/graphite [37]. $\theta_{Na} = 1$ ML corresponds to one Na adatom for every five surface C atoms, $\rho = 7.6 \times 10^{14}$ K atoms cm^{-2}.

No phase diagram is presented for Li on graphite, as no ordered overlayers were seen for $T = 90$ K [36, 26, 16]. It is possible that structures could be observed at much lower temperatures where intercalation will happen at a slower rate [16]. One report of a Li structure (after multilayer growth, annealing and cooling) suggests that a full monolayer of Li would have about twice the number of adatoms as the larger alkalis and about 30% more adatoms than an Na monolayer, i.e. $\rho \cong 10 \times 10^{14}$ Li atoms cm^{-2} [36].

6.2. The change in the electronic structure of the alkali metals and of the graphite upon adsorption

In principle, all alkali metal atoms are hydrogen-like, with pronounced tendency to transfer charge to the substrate. Still, their structural phases and intercalation capability are indicative of diverse electronic interactions with the substrate. Therefore, the understanding of the structure and properties of such adsorption systems benefits greatly from the awareness of the charge transferred between the adsorbed atoms and graphite. Table 4 brings together results of both experiments and theoretical calculations performed on various alkali metal/graphite systems, in different structural phases. The method employed and the estimated amount of charge transferred from the adatoms to the graphite substrate are specified for each structure.

Due to the abundance of work performed on K/graphite, there are several important features of this particular system which will be emphasized, as follows.

Table 4. The amount of charge per adsorbed atom, transferred to the graphite substrate, for various alkali metal–graphite systems. The results are obtained through experiments and/or theoretical calculations by the methods pointed out. 1 ML coverage corresponds to the (2×2) surface structure for all adsorption systems except for the Na/graphite in which case $\theta_{Na} = 1$ ML corresponds to a close-packed bcc Na plane (one Na atom per ≈5 C atoms).

Structure	Charge transferred per adatom	Method used
K/graphite dispersed phase [18, 41] $\theta < 0.1$ ML	$0.7e$	EELS + band structure calculations
K/graphite $\theta < 0.25$ ML Cs/graphite $\theta < 0.2$ ML Na/graphite $\theta < 1.25$ ML in dispersed phase [30]	0.4–0.5e 0.6–0.8e 0.1–0.2e	EELS + calculation based on the linear dependence of the alkali induced plasmon losses versus (coverage)$^{0.5}$
K/graphite in dispersed phase [5] $\theta < 0.3$ ML	$0.38 \pm 0.11e$	HREELS + dipole scattering theory applied to vibrating adatoms perpendicular to the graphite surface
K/graphite in dispersed phase [5] $\theta < 0.3$ ML	0.3–0.4e	Work function measurements (UPS & PD) + calculation of the charge associated with the dipole moment at the position of the adatoms
K/graphite in dispersed phase [8] $\theta < 0.38$ ML	0.5e	Work function measurements + calculation of the charge associated with the dipole moment at the position of the adatoms
Cs-(2×2)/graphite K–(2×2)/graphite Li/graphite for θ estimated between 1 and 3 ML Na/graphite at $\theta = 1 \pm 0.3$ ML K intercalated [26]	$0.9 \pm 0.1e$ $0.9 \pm 0.1e$ ≈1e <0.1e ≈1e	XPS + charge inferred from the energy shift of the graphite bands upon alkali adsorption
K/graphite In dispersed phase $\theta < 0.1$ ML K–(2×2) /graphite [19]	0.15–0.18e 0.012e	PES + rigid band model (shift of the Fermi level to fit exp. data)
Na/graphite at low coverage $\theta_{Na} = 0.2$ ML Na/graphite $\theta_{Na} = 1$ ML [38]	0.2e 0.04e	Photoemission from QWSs + rigid band model
K/graphite At $\theta = 0.25$ ML K–(2×2)/graphite [29]	0.28–0.38e 0.17–0.18e	First-principles total-energy calculations
K–(2×2)/graphite K–(4×4)/graphite [53]	0.17e 0.27–0.40e	First-principles methods within the density functional formalism
K/graphite At very low θ K/graphite $\theta = 0.25$ ML K–(2×2)/graphite [54]	0.64e 0.54e 0.46e	Cluster model solved within the framework of LSDA and GGA

- There is almost a consent regarding the nature of the adsorbate–substrate bonding in the case of K adsorbed on graphite. There are in principle two results [19, 26] that do not fit into the otherwise generally accepted picture. According to the majority of results [5, 8, 29, 30, 53, 54], though, it can be concluded that in the dispersed phase the charge transferred from the K atoms towards graphite is fairly large (with values of 0.3 up to 0.7e per adatom), indicating an ionic bond. As the coverage increases and the (2×2) islands start forming, the charge is redistributed within the K layer rather than

being transferred to the substrate, a fact illustrated by a drop in the calculated transferred charge down to values between 0.17e and 0.46e [29, 53, 54]. In the condensed phase, therefore, the K adlayer appears to have a metallic character.

- The transition itself from the dispersed to the condensed phase via islands that increase in dimension until, eventually, they cover the entire surface deserves to be mentioned as being representative for the K/graphite system. At the electronic level, the mechanisms responsible for keeping the adatoms as far apart as possible in the dispersed configuration are a Coulomb repulsive interaction between neighbouring K atoms which become ionized, and another repulsive effect due to the polarization of the graphite substrate reflecting its semimetallic character (in fact arising from the occupation of the graphite π^* bands with charge originating from K atoms), the so-called band-energy effect as described by Ishida and Palmer [27]. As the coverage increases, a decrease in the K–K distance becomes energetically too costly and the system evolves towards the formation of islands of close-packed adatoms. The repulsive-type interactions are partly counteracted by an attractive adatom–adatom interaction due to the overlap of the K 4s orbitals which contribute to the K metallic bond [52], in accordance with the idea that K in the (2×2) phase exhibits a metallic character.
- The cohesive energy of the K atoms in the (2×2) structure has been calculated to be larger than for K atoms in a (3×3) structure [52], also explained by a significant overlap of the 4s orbitals in the (2×2) case. This proves, even if for a singular case, why the (2×2) structure and not another one is observed experimentally.
- Also, a larger binding energy is calculated for isolated K atoms adsorbed on graphite as opposed to the reduced binding energy per adatom in the case of multiple K adsorption [54], in agreement with the idea of K–graphite charge transfer as a function of coverage. This serves as an argument for the hypothesis that K intercalation takes place from the dispersed phase, which would explain why the condensed phase is found to be more stable against intercalation than the dilute phase [5, 11].
- Ultimately, a multitude of intriguing experimental data such as the very small corrugation of the K–graphite surface potential [16, 20, 51], the change in work function with K coverage [5, 8, 10, 31], the photodesorption of the K adatoms [4, 7–9, 31], and features in the EELS, XPS and PES spectra [5, 8, 10, 11, 18, 19, 22, 26, 30, 41, 50], helped build the current understanding of the K–graphite interaction.

At the opposite pole, the charge transferred to the graphite substrate per Na atom is found to be very small, almost regardless of the coverage. Even if the results vary depending on the method applied, the charge transferred is never found to exceed 0.2e per adatom [26, 30, 38]. It appears that, unlike any other alkali metal, Na exists on the graphite surface in basically atomic form, having little interaction with the substrate. This lack of interaction may provide an explanation for why Na is so unlikely to form intercalation compounds [26].

Li, the smallest alkali metal atom, appears to easily intercalate even at temperatures as low as 100 K, a fact that would explain the large ionization potential inferred by the complete charge transfer found in an XPS study [26].

Although the problem of charge transfer has not been investigated for Rb/graphite and, in the case of Cs/graphite only few and somewhat conflicting data are available [26, 30], the similarity between the phase diagrams corresponding to these two adsorption systems and the phase diagram of K/graphite would imply similar adsorbate–substrate interactions. Still, additional experiments and calculations will have to decide.

6.3. Open problems

Without any claim on assembling an exhaustive list of unanswered questions concerning the alkali metals/graphite adsorption systems, several problems of interest worth investigating are presented below.

- The phases of K on graphite have been extensively studied in the past 20 years, while little investigation has been done on the other alkali metals adsorbed on graphite, by comparison (see section 6.1). The phase diagrams of Cs and Rb need information about the critical coverages that mark the phase transitions. Adsorption at more substrate temperatures should be investigated. There is also some controversy on the phases formed by Cs on graphite which should be resolved. Li and Na, on the other hand, due to their small size, are not expected to easily form superstructures as the other alkali metals. Still, an intriguing behaviour distinguishes between these two atomic species: Li atoms have a remarkable ability to intercalate while Na atoms rarely do so. Carefully chosen experimental conditions might challenge this behaviour.
- In the case of K on graphite, there is a general consent regarding the nature of the adsorbate–substrate bonding. Nevertheless, the actual amount of charge transferred at specific coverages, lies (both experimentally and theoretically) within too large a range (see section 6.2).
- Concerning other alkali metals adsorbed on graphite, the problem of charge transfer has either not yet been posed (as is the case of Cs and Rb), or it has been little studied and a conclusion is hard to draw due to a lack of statistically significant number of results (see section 6.2).
- Significant information concerning the electronic structure of these adsorption systems can be obtained from electron energy spectroscopy as well as from photoemission studies. The attribution of the EELS loss features to specific electronic excitations, and monitoring these electronic excitations as a function of coverage are necessary steps in explaining the process of adsorption at electronic (thus fundamental) level. Of similar importance is the observation of the alkali-induced plasmon excitation of graphite, which shifts in energy as a function of alkali coverage. Interestingly (and not yet explained), the plasmon feature reaches an energy limit which happens to be the same for K, Cs or Na on graphite (see section 5.1.1). Few photoemission studies have been reported and, as far as K–graphite charge transfer is concerned, their findings do not coincide (see sections 5.1.2 and 6.2). Alkali metal/graphite adsorption systems would greatly benefit from additional EELS and photoemission experiments.

Acknowledgments

We thank R D Diehl and D Chakarov for helpful discussions and comments. Also, the comments of the referees were greatly appreciated.

References

[1] Dresselhaus M S and Dresselhaus G 1981 *Adv. Phys.* **30** 139
[2] Inagaki M 2001 *Graphite and Precursors* vol 1, ed P Delhaes (Amsterdam: Gordon and Breach) p 179
[3] Wu N J and Ignatiev A 1982 *Phys. Rev.* B **25** 2983–6
[4] Chakarov D V, Österlund L, Hellsing B and Kasemo B 1996 *Appl. Surf. Sci.* **106** 186
[5] Österlund L, Chakarov D V and Kasemo B 1999 *Surf. Sci.* **420** 174

[6] Wandelt K 1989 *Physics and Chemistry of Alkali Metal Adsorption* vol 57, ed H P Bonzel, A M Bradshaw and G Ertl (Amsterdam: Elsevier) p 25
[7] Hellsing B, Chakarov D V, Österlund L, Zhdanov V P and Kasemo B 1996 *Surf. Sci.* **363** 247
[8] Hellsing B, Chakarov D V, Österlund L, Zhdanov V P and Kasemo B 1997 *J. Chem. Phys.* **106** 982
[9] Chakarov D V, Österlund L, Hellsing B, Zhdanov V P and Kasemo B 1994 *Surf. Sci.* **311** L724
[10] Hock K M and Palmer R E 1993 *Surf. Sci.* **284** 349
[11] Barnard J C, Hock K M and Palmer R E 1993 *Surf. Sci.* **287/288** 178
[12] Sjövall P 1996 *Surf. Sci.* **345** L39
[13] Hu Z P, Li J, Wu N J and Ignatiev A 1989 *Phys. Rev.* B **39** 13201
[14] Hu Z P, Wu N J and Ignatiev A 1986 *Phys. Rev.* B **33** 7683
[15] Diehl R D and McGrath R 1996 *Surf. Sci. Rep.* **23** 43
[16] White J D 1994 *PhD Thesis* The Pennsylvania State University, University Park, p 153
[17] Wu N J and Ignatiev A 1983 *Phys. Rev.* B **28** 7288
[18] Li Z Y, Hock K M and Palmer R E 1991 *Phys. Rev. Lett.* **67** 1562
[19] Bennich P, Puglia C, Brühwiler P A, Nilsson A, Maxwell A J, Sandell A, Mårtensson N and Rudolf P 1999 *Phys. Rev.* B **59** 8292
[20] Cui J, White J D, Diehl R D, Annett J F and Cole M W 1992 *Surf. Sci.* **279** 149
[21] Ferralis N, Pussi K, Finberg S E, Smerdon J, Lindroos M, McGrath R and Diehl R D 2004 *Phys. Rev.* B **70** 245407
[22] Breitholtz M, Kihlgren T, Lindgren S-Å and Walldén L 2002 *Phys. Rev.* B **66** 153401
[23] Bacon G E 1948 *Acta Crystallogr.* **1** 337
[24] Wu N J and Ignatiev A 1982 *J. Vac. Sci. Technol.* **20** 896
[25] Pussi K, Smerdon J, Ferralis N, Lindroos M, McGrath R and Diehl R D 2004 *Surf. Sci.* **548** 157
[26] Johnson M T, Starnberg H I and Hughes H P 1986 *Surf. Sci.* **178** 290
[27] Ishida H and Palmer R E 1992 *Phys. Rev.* B **46** 15484–9
[28] Wertheim G K, Riffe D M and Citrin P H 1994 *Phys. Rev.* B **49** 4834–41
[29] Ancilotto F and Toigo F 1993 *Phys. Rev.* B **47** 13713
[30] Gleeson M, Kasemo B and Chakarov D 2003 *Surf. Sci.* **524** L77
[31] Breitholtz M, Algdal J, Kihlgren T, Lindgren S-Å and Walldén L 2004 *Phys. Rev.* B **70** 125108
[32] Hunt M R C, Durston P J and Palmer R E 1996 *Surf. Sci.* **364** 266
[33] Novaco A D and McTague J P 1977 *Phys. Rev. Lett.* **38** 1286
[34] Wu N J, Hu Z P and Ignatiev A 1991 *Phys. Rev.* B **43** 3805
[35] Chakarov D V 2005 private communication
[36] Hu Z P and Ignatiev A 1984 *Phys. Rev.* B **30** 4856
[37] Breitholtz M, Kihlgren T, Lindgren S-Å, Olin H, Wahlström E and Walldén L 2001 *Phys. Rev.* B **64** 073301
[38] Breitholtz M, Kihlgren T, Lindgren S-Å and Walldén L 2003 *Phys. Rev.* B **67** 235416
[39] Rytkonen K, Akola J and Manninen M 2004 *Phys. Rev.* B **69** 205404
[40] Dresselhaus M S, Dresselhaus G and Saito R 2001 *Graphite and Precursors* vol 1, ed P Delhaes (Amsterdam: Gordon and Breach) p 25
[41] Li Z Y, Hock K M, Palmer R E and Annett J F 1991 *J. Phys.: Condens. Matter* **3** 103
[42] Swan J B 1964 *Phys. Rev.* **135** A1467–70
[43] Jensen E T, Palmer R E, Allison W and Annett J F 1991 *Phys. Rev. Lett.* **66** 492–5
[44] Tatar R C and Rabii S 1982 *Phys. Rev.* B **25** 4126–41
[45] Ritchie R H 1957 *Phys. Rev.* **106** 874–81
[46] Andersson S, Persson B N J, Gustafsson T and Plummer E W 1980 *Solid State Commun.* **34** 473
[47] Woodruff D P and Delchar T A 1994 *Modern Techniques of Surface Science* (Cambridge: Cambridge University Press)
[48] Feuerbacher B and Fitton B 1972 *J. Appl. Phys.* **43** 1563
[49] Fretigny C, Marchand D and Laguës M 1985 *Phys. Rev.* B **32** 8462–4
[50] Sandell A, Hjortstam O, Nilsson A, Brühwiler P A, Eriksson O, Bennich P, Rudolf P, Wills J M, Johansson B and Mårtensson N 1997 *Phys. Rev. Lett.* **78** 4994–7
[51] White J D, Cui J, Strauss M, Diehl R D, Ancilotto F and Toigo F 1994 *Surf. Sci.* **307–309** 1134
[52] Hjortstam O, Wills J M, Johansson B and Eriksson O 1998 *Phys. Rev.* B **58** 13191
[53] Lamoen D and Persson B N J 1998 *J. Chem. Phys.* **108** 3332
[54] Lou L, Österlund L and Hellsing B 2000 *J. Chem. Phys.* **112** 4788
[55] Johnson M T, Starnberg H I and Hughes H P 1986 *Solid State Commun.* **57** 545